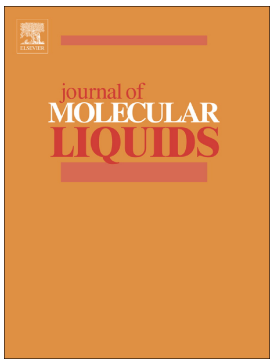

Synthesis and properties of symmetrical N,N′-bis(alkyl)imidazolium bromotrichloroferrate(III) paramagnetic, room temperature ionic liquids with high short-term thermal stability

Kevin T. Greeson, Nicolas G. Hall, Neil D. Redeker, Jacob C. Marcischak, Laina V. Gilmore, Jerry A. Boatz, Tammy C. Le, Jeffrey R. Alston, Andrew J. Guenthner, Kamran B. Ghiassi

PII: S0167-7322(18)30957-7
DOI: doi:10.1016/j.molliq.2018.06.016
Reference: MOLLIQ 9214

To appear in: *Journal of Molecular Liquids*

Received date: 23 February 2018
Revised date: 1 June 2018
Accepted date: 5 June 2018

Please cite this article as: Kevin T. Greeson, Nicolas G. Hall, Neil D. Redeker, Jacob C. Marcischak, Laina V. Gilmore, Jerry A. Boatz, Tammy C. Le, Jeffrey R. Alston, Andrew J. Guenthner, Kamran B. Ghiassi , Synthesis and properties of symmetrical N,N′-bis(alkyl)imidazolium bromotrichloroferrate(III) paramagnetic, room temperature ionic liquids with high short-term thermal stability. Molliq (2017), doi:10.1016/j.molliq.2018.06.016

Synthesis and properties of symmetrical *N*,*N*'-bis(alkyl)imidazolium bromotrichloroferrate(III) paramagnetic, room temperature ionic liquids with high short-term thermal stability

Kevin T. Greeson,[1] Nicolas G. Hall,[1] Neil D. Redeker,[1] Jacob C. Marcischak,[2] Laina V. Gilmore,[1] Jerry A. Boatz,[2] Tammy C. Le,[1] Jeffrey R. Alston,[1,3] Andrew J. Guenthner,[2,4] Kamran B. Ghiassi[2]*

[1] ERC, Incorporated, Air Force Research Laboratory, Edwards AFB, CA 93524, USA

[2] Air Force Research Laboratory, Aerospace Systems Directorate, Edwards AFB, CA 93524, USA

[3] Joint School of Nanoscience and Nanoengineering, North Carolina A&T State University, Greensboro, NC 27401, USA

[4] Nano Hydrophobics Inc., Lawrence Berkeley National Laboratory, Berkeley, CA 94720, USA

ABSTRACT

A series of paramagnetic ionic liquids (PILs) based on *N*,*N*'-bis(alkyl)imidazolium bromotrichloroferrate(III), $[(C_n)_2Im][FeCl_3Br]$ (Im = imidazole; C_n = ethyl, butyl, hexyl, octyl, decyl, dodecyl), was prepared and compared against the more traditional $[C_nC_1Im][FeCl_3Br]$ (C_1 = methyl) analogs. Both series were extensively characterized by physical, chemical, and computational methods including differential scanning calorimetry (DSC), thermogravimetric analysis (TGA), spectroscopy (FTIR and UV-vis-NIR), magnetic susceptibility, surface tensiometry, density, and viscosity. The X-ray crystal structure of $[(C_{12})_2Im][FeCl_3Br]$ was also obtained. Notably, all ionic liquids prepared in this study show short-term thermal stabilities exceeding 300 °C in air and have melting points equal to or lower than 25 °C, which is surprisingly low for ionic

liquids containing symmetrical cations. In addition, all presented ionic liquids have relatively low viscosities allowing for easier transitioning into applications. Physical property trends are discussed.

KEYWORDS

Ionic liquid, imidazolium, symmetry, thermal stability, magnetism, crystallography

INTRODUCTION

Ionic liquids (ILs) have recently come to represent an important class of compounds due to their versatility in applications and materials chemistry. Conventionally, ionic liquids are defined as salts with melting points below 100 °C, although room temperature ionic liquids (RTILs) are often further specified when the substance is a liquid under standard laboratory conditions.[1-2] ILs have been utilized as reaction solvents, extraction media for environmental toxins, and even as crystal engineering agents for pharmaceutical applications.[1-9] The extremely low vapor pressure of ILs also provides the potential for use at elevated temperatures without the hazards and instabilities associated with evaporation, although this particular aspect of IL applications has received less attention.

Among the many varieties of ILs, paramagnetic ionic liquids (PILs or MILs) are relatively new and less explored.[10] These species commonly derive their magnetic properties from anion complexation with transition metals (Mn, Fe, Co, Cu) or rare-earth metals (Eu, Gd, Dy) with unpaired electrons.[11-16] Since many ionic liquids contain a halide as the anion, a facile addition of metal halide will generate the corresponding PIL. The most common cations for PILs include

quaternary ammonium, imidazolium, pyridinium, and pyrrolidinium while the most common anion is tetrachloroferrate(III), $[FeCl_4]^-$.[5, 10, 17-18] From an inorganic and magnetic perspective, $[FeCl_4]^-$ is a perfect tetrahedral (T_d), high-spin d^5 ion. Since halides are common ligands in transition metal chemistry, the utilization of these transition metal halides is fairly intuitive. However, there are a few reports of metal-free paramagnetic ionic liquids.[18]

PILs have been investigated as process liquids for catalysis, cellulose degradation, gas adsorption, microfluidic processing, and extraction.[6, 10] Of note, the Whitesides group invented a method using PILs for density determination via magnetic levitation.[19] In most of these cases, the PIL serves mainly as a carrier fluid with interesting magnetic properties. The potential for enhanced stability at high temperatures, however, affords the opportunity for PILs to perform as multi-functional liquids in high temperature environments. These performance characteristics could facilitate a wide variety of relatively unexplored applications for these materials in electronics, aerospace, and power generation applications. For instance, PILs that can survive high temperatures for short periods of time, possess low viscosities, and have relatively low surface tension could serve as heat-transfer fluids with magnetically-controlled convection.

To facilitate the exploration of these possibilities, two series of *N*,*N*'-substituted imidazolium-based ionic liquids were investigated. Herein we report the synthesis, characterization, and properties for two series of alkylated PILs, $[(C_n)_2Im][FeCl_3Br]$ and $[C_nC_1Im][FeCl_3Br]$ (Im = imidazole; C_1 = methyl; C_n = 2 (ethyl), 4 (butyl), 6 (hexyl), 8 (octyl), 10 (decyl), 12 (dodecyl). Of note, we observed that the $[(C_n)_2Im][FeCl_3Br]$ compounds were all room temperature ionic liquids. Nonetheless, the crystal structure of $[(C_{12})_2Im][FeCl_3Br]$ was also obtained. Comprehensive thermal and physical characterization including differential scanning

calorimetry (DSC), thermogravimetric analysis (TGA), spectroscopy (FTIR and UV-vis-NIR), magnetic susceptibility, surface tensiometry, density, and viscosity revealed remarkable short-term thermal stability above 300 °C in air with relatively low viscosity and surface tension values compared to other ionic liquids (it is important to note that the term "thermal stability" does not have a single or consistent definition.[48] With regard to the work presented here, "short-term thermal stability" refers to the temperature at which the decomposition onset is measured as 5% weight loss under ramped temperature experiments). Additionally, theoretical calculations of the gas-phase enthalpies and free energies for the synthesis of both series of PILs from the addition of $FeCl_3 \bullet 6H_2O$ to the bis(alkyl)imidazolium bromide precursor were performed. These materials therefore represent promising candidates for new and important applications of ILs where these special characteristics are required.

RESULTS AND DISCUSSION

Synthesis. The 1-alkyl-3-methylimidazolium bromide intermediates, $[C_nC_1Im]Br$ (C_n = 2, 4, 6, 8, 10, 12) are prepared readily by reacting 1-methylimidazole with 1-bromoalkane either neat or in acetonitrile under reflux conditions.[9, 20-21] The preparation of symmetrical, bis-alkylated imidazolium intermediates, $[(C_n)_2Im]X$ (C_n = 2, 4, 6, 8, 10, 12; X = Cl or Br), typically involves *in situ* treatment of imidazole with sodium hydride followed by two equivalents of alkyl halide.[22] An alternative synthesis involves the *in situ* reaction of imidazole with a base, such as potassium carbonate or potassium hydroxide.[23-24] Halides such as chloride and bromide are commonly used, although iodide salts are also reported.[20] Alkyl bromides were chosen for this study due to cost, incorporation of a better leaving group, and to allow further reaction with $FeCl_3 \bullet 6H_2O$ (*vide*

infra). We explored a different synthesis path involving the treatment of imidazole with sodium hydroxide to produce the sodium imidazolate salt, NaIm, prior to reacting with the alkyl bromide. This eliminates the need for strict anaerobic reaction conditions, such as those required when handling sodium hydride (Scheme 1). This precursor, NaIm, can be stored excluding light and moisture for months.[25] The reaction of NaIm proceeds in the same manner as the sodium hydride reduction of imidazole, requiring two equivalents of alkyl bromide in tetrahydrofuran. Although the yields are comparable, but not as high as other literature methods, this route does verify NaIm as a viable starting material.

Both series $[(C_n)_2Im][FeCl_3Br]$ and $[C_nC_1Im][FeCl_3Br]$ (C_n = 2, 4, 6, 8, 10, 12) can be prepared by mixing equimolar amounts of imidazolium bromide and $FeCl_3 \bullet 6H_2O$ under an atmosphere of nitrogen.[26] Anhydrous $FeCl_3$ can be utilized as well, but the reaction conditions become more cumbersome due to the anaerobic conditions needed to store $FeCl_3$.[27-28] These preparation methods are analogous for the synthesis of asymmetric imidazolium tetrahaloferrate(III) compounds (e.g. $[C_4C_1Im][FeCl_4]$ also referred to as [BMIm][$FeCl_4$]).[27] The entire $[C_nC_1Im][FeCl_4]$ analogs have been synthesized previously, along with only one $[(C_n)_2Im][FeCl_4]$ compound, $[(C_4)_2Im][FeCl_4]$, leaving almost the entire symmetrical series unexplored.[7, 29-33] In addition, relatively little work has been reported using the $[FeCl_3Br]^-$ anion.[7, 33] The specific compounds prepared for those studies were $[C_4C_1Im][FeCl_3Br]$ and $[C_6C_1Im][FeCl_3Br]$, focusing on sulfur extraction of fuels and regioselective benzylation.[7, 33] Consequently, no physical or thermal property data were reported. This gap prompted us to explore both series with the $[FeCl_3Br]^-$ anion.

For facile synthesis, we used the iron(III) chloride hexahydrate starting material. The full reaction is shown in Scheme 1. The reactions can be performed neat under a blanket of nitrogen for the entire $[C_nC_1Im][FeCl_3Br]$ series and for C_n = 2, 4, 6, 8, and 10 of the $[(C_n)_2Im][FeCl_3Br]$ series, owing to the fact that the products are liquids at room temperature (25 °C). For the remaining compound, $[(C_{12})_2Im][FeCl_3Br]$, a solvent (methanol) was utilized to allow for proper mixing since the product is solid at room temperature. After a sufficient amount of stirring, water and solvents can be removed by vacuum while heating.

Scheme 1. Synthetic pathway for the preparation of $[(C_n)_2Im][FeCl_3Br]$ and $[C_nC_1Im][FeCl_3Br]$.

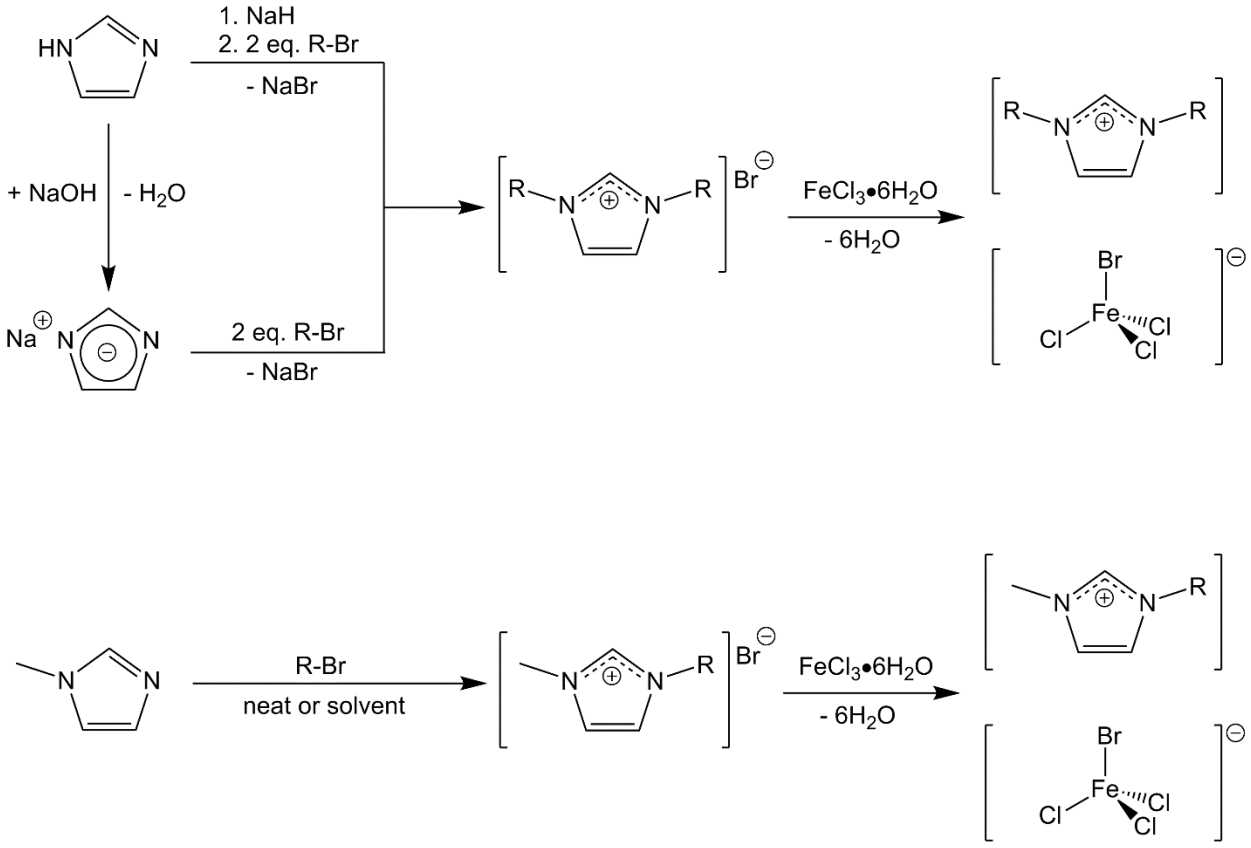

Physical Properties. Table 1 shows physical properties and thermal data tabulated from differential scanning calorimetry (DSC), thermogravimetric analysis (TGA), density, viscosity, surface tensiometry, and magnetic susceptibility experiments. For this study, a standard Schlenk line and oil heating bath (10^{-2} torr and 80 °C, respectively) were utilized to remove residual water, after which the products were stored under an atmosphere of nitrogen in a desiccator (phosphorous pentoxide as desiccant) until measurement. The samples were verified to be free of water via TGA, using weight loss after 1 hour at 110 °C as an estimate for volatiles content. All samples were dried until the estimated water content was <0.5% (Supporting Information). As expected, for both series, the density at 25 °C (plotted as a function of linear alkyl chain length, *n*, in Figure 1) decreases as the alkyl group size increases. In addition, the $[C_nC_1Im][FeCl_3Br]$ compounds have higher density values than their $[(C_n)_2Im][FeCl_3Br]$ counterparts due to the lower volume fraction of alkyl groups for an identical value of *n*. More specifically, the density are described very well by a group contribution model of molar volume in which each methylene segment contributes 16.8 ± 0.2 $cm^3\ mol^{-1}$, with the remainder of each molecule contributing 198.7 ± 1.7 $cm^3\ mol^{-1}$. These values were determined by a linear regression of molar volume on the number of methylene groups, that is, *n*-1 for the $[C_nC_1Im][FeCl_3Br]$ compounds and 2(*n*-1) for the $[(C_n)_2Im][FeCl_3Br]$ compounds. This group contribution value for methylene segments may include contributions from both the actual volume required to add the segment, as well as a small positive contribution due to the decrease in ion density associated with the addition of each segment.

The kinematic viscosity values (25 °C) for both series also behave as expected. Viscosity increases as a function of alkyl chain length. While the $[C_nC_1Im][FeCl_3Br]$ series viscosity values

gradually rise to 87 cSt, the $[(C_n)_2Im][FeCl_3Br]$ compounds rise sharply in comparison to 212 cSt, as illustrated in Figure 2. These increases are mainly driven by increasing molecular size characteristics, with the $[(C_n)_2Im][FeCl_3Br]$ compounds being considerably larger for the same value of *n* due to their two-armed architecture.

Surface tension values (25 °C) for both series were determined using the pendant drop method[34-35] and are shown in Figure 3 as a function of alkyl chain length. The $[C_nC_1Im][FeCl_3Br]$ compounds have higher surface tension values compared to the $[(C_n)_2Im][FeCl_3Br]$ analogs, ranging from 33.8 to 52.3 mN m^{-1}. However, the $[(C_n)_2Im][FeCl_3Br]$ are quite close ranging from 29.2 to 50.5 mN m^{-1}. Both series decrease in surface tension as alkyl chain length increases. The lowest value observed, 29.2 mN m^{-1} for $[(C_{12})_2Im][FeCl_3Br]$, is characteristic of long-chain alkanes that includes some polar moieties, such as 1-decanol (29.6 mN m^{-1} at 10 °C)

Solubilities were determined for both series using hexanes, toluene, dichloromethane, chloroform, tetrahydrofuran, diethyl ether, acetone, acetonitrile, methanol, and water. The results are presented in Table 2. It is interesting to note that both series are insoluble in hexanes and display solubility in the remaining nine solvents. Other reports of similar compounds have labeled this class of PILs as "magnetic surfactants."[36] However, to our knowledge, this is the first report focusing on symmetrical $[(C_n)_2Im][FeCl_3Br]$ imidazolium species, possibly owing to the generally higher melting points found in symmetrical species.[37] It is therefore intriguing that we were able to produce RTILs with symmetrical alkylated species.

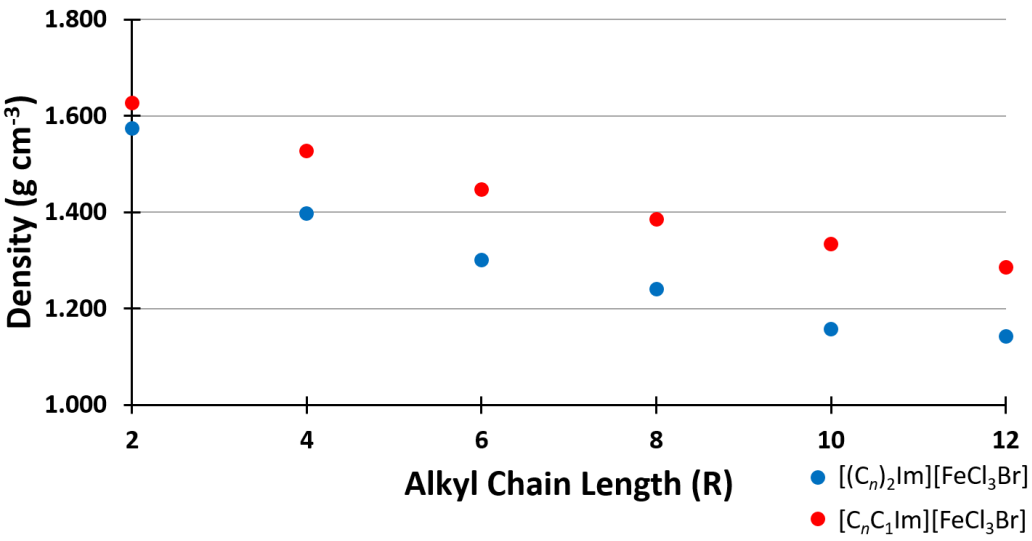

Figure 1. Density plot as a function of alkyl chain length for the $[(C_n)_2Im][FeCl_3Br]$ and $[C_nC_1Im][FeCl_3Br]$ series.

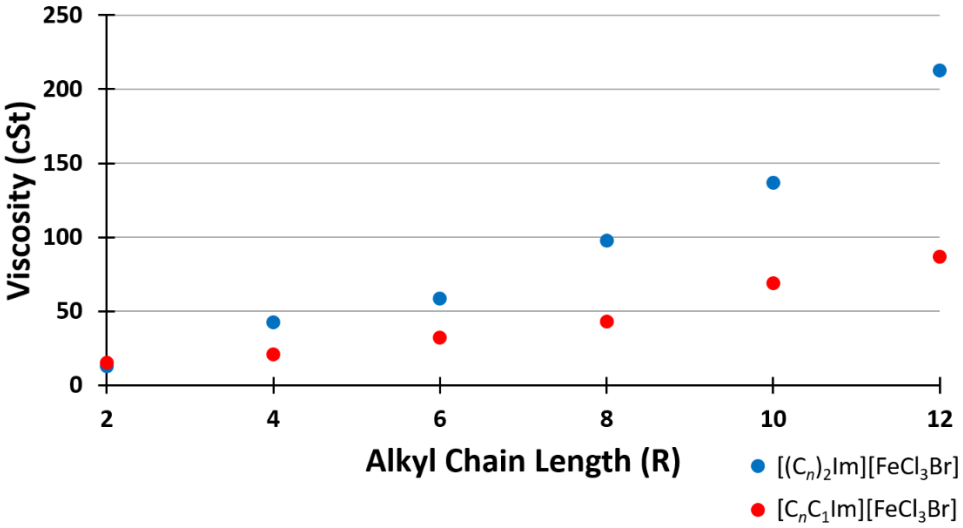

Figure 2. Viscosity plot as a function of alkyl chain length for the $[(C_n)_2Im][FeCl_3Br]$ and $[C_nC_1Im][FeCl_3Br]$ series.

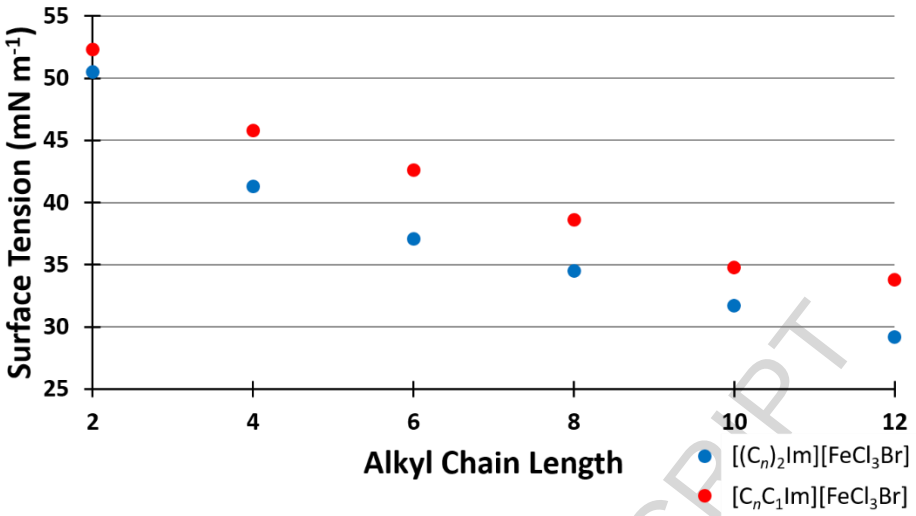

Figure 3. Surface tension plot as a function of alkyl chain length for the $[(C_n)_2Im][FeCl_3Br]$ and $[C_nC_1Im][FeCl_3Br]$ series.

Table 1. Physical and thermal properties of the $[(C_n)_2Im][FeCl_3Br]$ and $[C_nC_1Im][FeCl_3Br]$ series.

Compound	density (g cm^{-3})[a]	viscosity (cSt)[b]	surface tension (mN m^{-1})[c]	melting point (°C)[d]	short-term thermal stability (°C)[e]	χ_{mol} (m^3 mol^{-1} x 10^{-7})	μ_{eff} (μ_B)
$[(C_2)_2Im][FeCl_3Br]$	1.573	12.8	50.5	–0.1	331	1.77	5.73
$[(C_4)_2Im][FeCl_3Br]$	1.397	42.6	41.3	--	310	1.76	5.71
$[(C_6)_2Im][FeCl_3Br]$	1.300	58.7	37.1	--	307	1.76	5.69
$[(C_8)_2Im][FeCl_3Br]$	1.241	97.8	34.5	--	300	1.73	5.65
$[(C_{10})_2Im][FeCl_3Br]$	1.158	136.9	31.7	4.6	305	1.75	5.69
$[(C_{12})_2Im][FeCl_3Br]$	1.142	212.5	29.2	25.1	309	1.79	5.75
$[C_2C_1Im][FeCl_3Br]$	1.627	15.2	52.3	19.4	327	1.78	5.73
$[C_4C_1Im][FeCl_3Br]$	1.527	21.1	45.8	--	335	1.73	5.64
$[C_6C_1Im][FeCl_3Br]$	1.447	32.4	42.6	--	318	1.76	5.71
$[C_8C_1Im][FeCl_3Br]$	1.385	43.0	38.6	--	311	1.78	5.73
$[C_{10}C_1Im][FeCl_3Br]$	1.334	69.2	34.8	-9.4	315	1.73	5.65
$[C_{12}C_1Im][FeCl_3Br]$	1.286	86.8	33.8	14.5	307	1.70	5.60

a. Density measured at 25 °C.
b. Kinematic viscosity at 25 °C.
c. Surface tension determined from pendant drop method at 25 °C.

d. Melting point determined via DSC endotherm and verified via visual melting point determination. In several cases, denoted by --, melting points could not be observed via either measurement method.
e. TGA temperature (air, 5 °C/min) at which 5 wt% loss of compound is observed.

Table 2. Solubility profile for the $[(C_n)_2Im][FeCl_3Br]$ and $[C_nC_1Im][FeCl_3Br]$ series.

	hexanes	toluene	CH_2Cl_2	$CHCl_3$	THF	ether	acetone	CH_3CN	CH_3OH	H_2O
$[(C_2)_2Im][FeCl_3Br]$	N	P	Y	Y	Y	P	Y	Y	Y	P
$[(C_4)_2Im][FeCl_3Br]$	N	P	Y	Y	Y	P	Y	Y	Y	P
$[(C_6)_2Im][FeCl_3Br]$	N	P	Y	Y	Y	Y	Y	Y	Y	P
$[(C_8)_2Im][FeCl_3Br]$	N	Y	Y	Y	Y	Y	Y	Y	Y	P
$[(C_{10})_2Im][FeCl_3Br]$	N	Y	Y	Y	Y	Y	Y	Y	Y	Y
$[(C_{12})_2Im][FeCl_3Br]$	N	Y	Y	Y	Y	Y	Y	Y	Y	Y*
$[C_2C_1Im][FeCl_3Br]$	N	Y	Y	Y	Y	Y	Y	Y	Y	Y
$[C_4C_1Im][FeCl_3Br]$	N	Y	Y	Y	Y	Y	Y	Y	Y	Y
$[C_6C_1Im][FeCl_3Br]$	N	Y	Y	Y	Y	Y	Y	Y	Y	Y
$[C_8C_1Im][FeCl_3Br]$	N	Y	Y	Y	Y	Y	Y	Y	Y	Y
$[C_{10}C_1Im][FeCl_3Br]$	N	Y	Y	Y	Y	Y	Y	Y	Y	Y
$[C_{12}C_1Im][FeCl_3Br]$	P/N	Y	Y	Y	Y	Y	Y	Y	Y	Y

Y = soluble; N = insoluble; P = partially soluble; * = emulsion

Magnetic susceptibility. Due to the low cost and abundance of iron, the paramagnetic nature of d^5 iron(III) has drawn considerable attention. Many reports have shown paramagnetism at room temperature, with high susceptibility to external magnets such as $Nd_2Fe_{14}B$ and even lower strength fields.[10, 17, 19, 26-27, 30, 36, 38] From an applications standpoint, this makes chemical extraction quite appealing especially in biphasic systems. For this study, magnetic susceptibility was measured using an Evans balance. The molar magnetic susceptibility (χ_{mol}) can be measured using the standard equation:

$$\chi_{mol} = \frac{C_{bal} L M (R - R_0)}{10^9 m} \quad \text{(Eq. 1)}$$

where C_{bal} is a balance calibration constant, L is the length of the sample in the tube, M is the molar mass, R is the instrument reading, R_0 is the instrument reading of the unloaded tube, and m is the sample mass. With χ_{mol} determined, the effective magnetic moment (μ_{eff}) can also be readily calculated at the measured temperature, T:

$$\mu_{eff} = 2.828\sqrt{\chi_{mol} \mathrm{T}} \quad \text{(Eq. 2)}$$

For the [$(C_n)_2$Im][$FeCl_3Br$] series, the μ_{eff} values range from 5.65 to 5.75 μ_B. The [C_nC_1Im][$FeCl_3Br$] series have similar values ranging from 5.60 to 5.73 μ_B. For reference, the reported μ_{eff} for the representative compound [C_4C_1Im][$FeCl_4$] is 5.90 μ_B.[15, 30] Similar values have been reported for [C_8C_1Im][$FeCl_4$] and [$C_{10}C_1$Im][$FeCl_4$], with corresponding μ_{eff} values of 5.78 and 5.66 μ_B, respectively.[15, 30] When added to hexanes, we have demonstrated that all of the prepared PILs in this study can be manipulated by an external magnetic field, as shown in Figure 4.

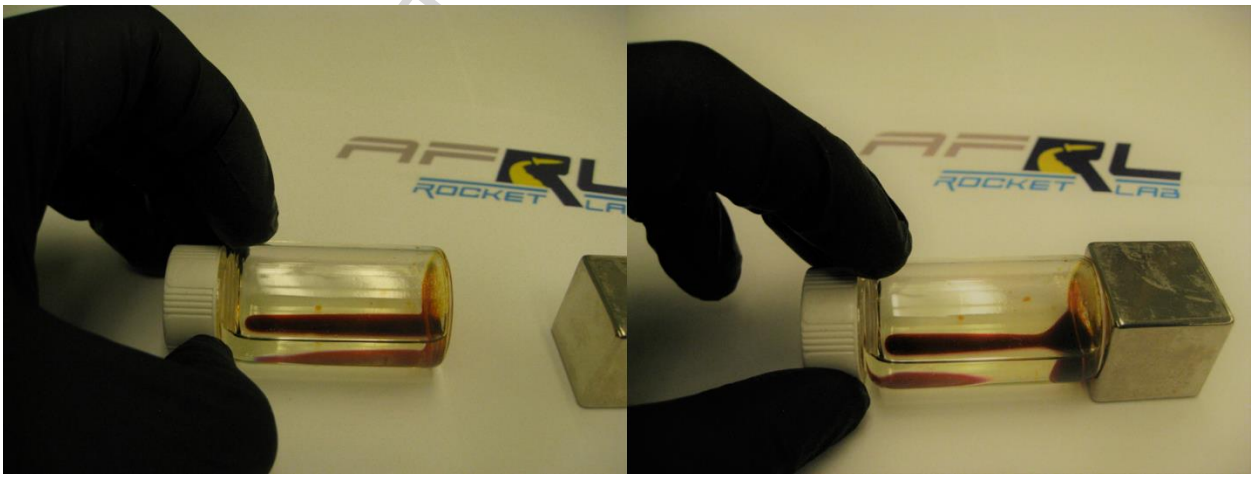

Figure 4. Photographs of [$C_{12}C_{12}$Im][$FeCl_3Br$] showing the immiscibility in hexanes (left) and magnetic susceptibility (right).

Thermal Properties. The prepared PILs were examined using differential scanning calorimetry (DSC) and thermogravimetric analysis (TGA). The second-heat DSC traces are shown in Figures 5 and 6 for $[(C_n)_2Im][FeCl_3Br]$ and $[C_nC_1Im][FeCl_3Br]$, respectively.

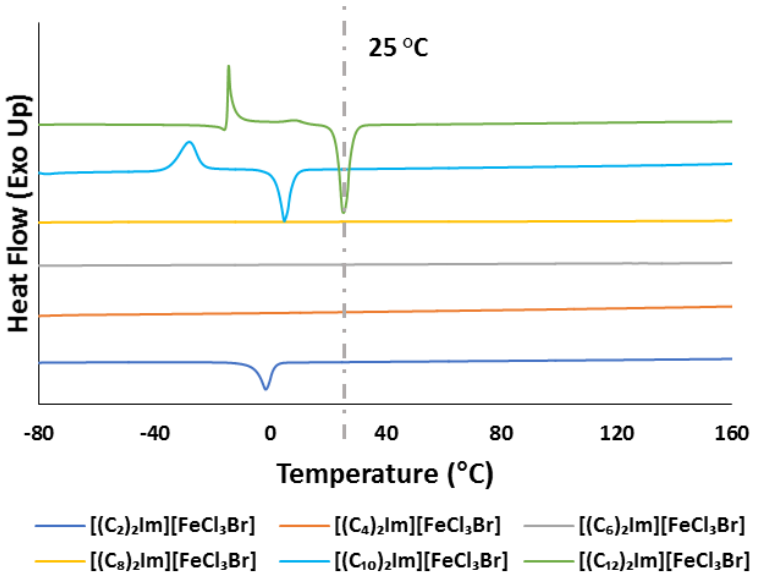

Figure 5. Compiled second-heat DSC traces of the $[(C_n)_2Im][FeCl_3Br]$ series. The *y* axis has been offset vertically for clarity. A dashed line is shown to represent conventional ambient temperature (25 °C).

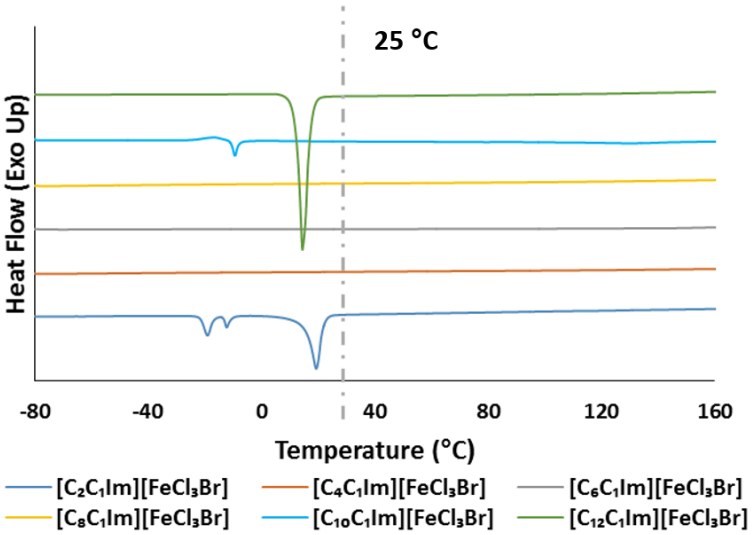

Figure 6. Compiled second-heat DSC traces of the $[C_nC_1Im][FeCl_3Br]$ series. The *y* axis has been offset vertically for clarity. A dashed line is shown to represent conventional ambient temperature (25 °C).

The DSC heat curves indicate the presence of crystalline melting transitions for C_2, C_{10}, and C_{12} species in both the $[C_nC_1Im][FeCl_3Br]$ and $[(C_n)_2Im][FeCl_3Br]$ series. Under the given experimental conditions, no crystalline melt was observed for the C_4, C_6 and C_8 compounds in either series. Further investigation via visual melting point determination confirmed these results. Curiously, there is not a dramatic difference in melt temperatures between the $[C_nC_1Im][FeCl_3Br]$ and $[(C_n)_2Im][FeCl_3Br]$ series; we observed less than 15 °C difference in melting point between the symmetric and asymmetric species. This may be due to the bulky nature of the $[FeCl_3Br]^-$ anion, which could disrupt alkyl chain crystallization.[37]

Figures 7 and 8 show combined TGA plots for the $[(C_n)_2Im][FeCl_3Br]$ and $[C_nC_1Im][FeCl_3Br]$ series, respectively. All compounds show excellent short-term thermal stability with onset of degradation exceeding 300 °C in air for all cases. Short-term thermal stability appears to be

inversely correlated with alkyl chain length in both $[(C_n)_2Im][FeCl_3Br]$ and $[C_nC_1Im][FeCl_3Br]$ series, likely due to the overall decrease in ionic character of the species as alkyl chain length increases. The degradation mechanisms for both series are quite complex, as indicated by the multiple steps in each compound's trace. This multistep degradation behavior is also observed with the $[C_nC_1Im][FeCl_4]$ series reported by Zhou and coworkers.[29]

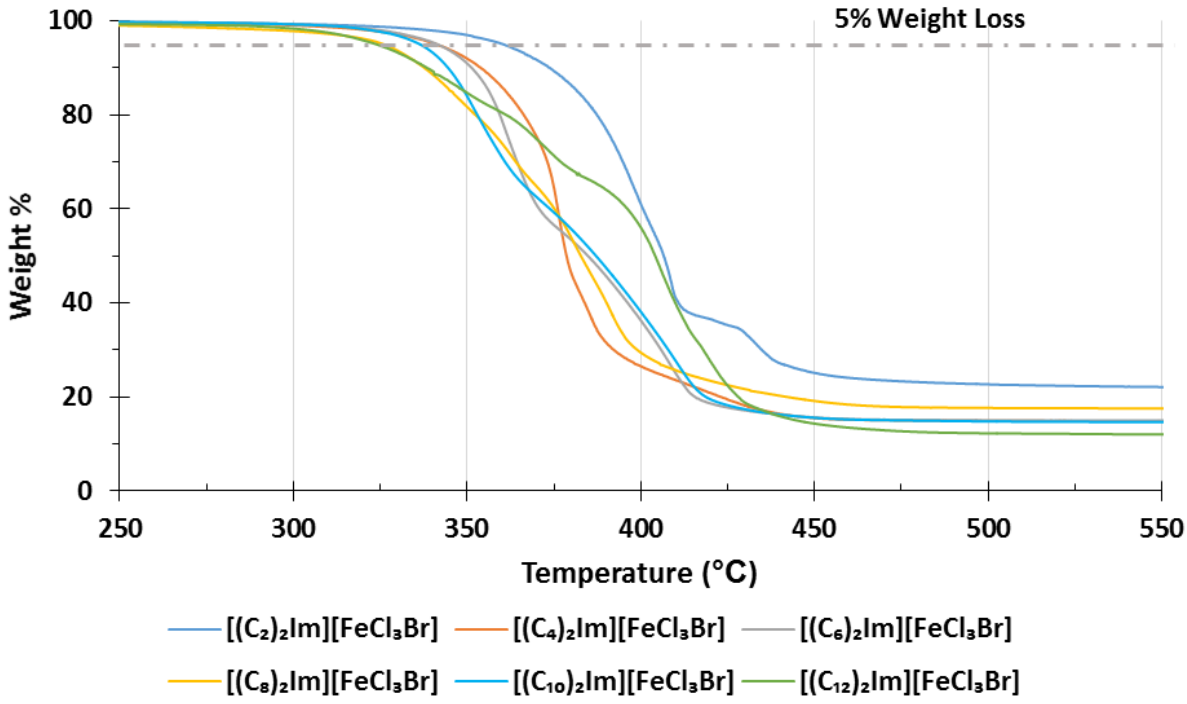

Figure 7. TGA plot for the $[(C_n)_2Im][FeCl_3Br]$ series in air. A dashed line is shown to aid the representation for 5% weight loss. Heating ramp rate was performed at 5 °C/min after an isothermal temperature hold at 110 °C for one hour.

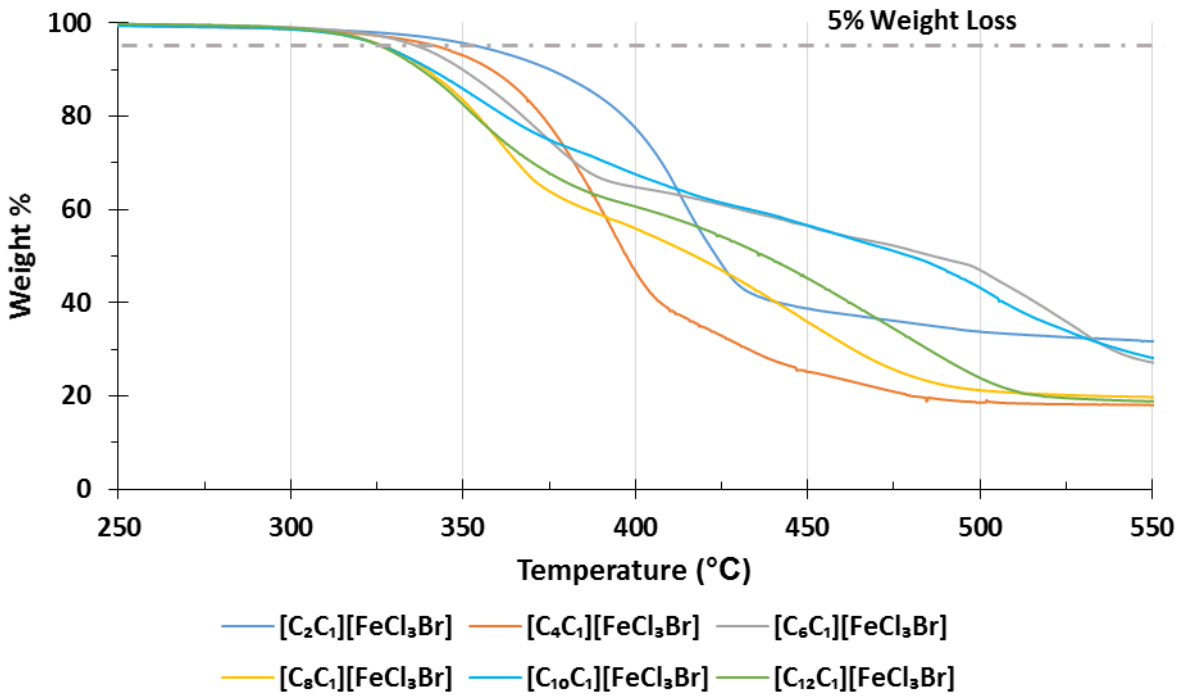

Figure 8. TGA plot for the [C_nC_1Im][$FeCl_3Br$] series in air. A dashed line is shown to aid the representation for 5% weight loss. Heating ramp rate was performed at 5 °C/min after an isothermal temperature hold at 110 °C for one hour.

Crystal Structure of [$(C_{12})_2$Im][$FeCl_3Br$]. Crystals of [$(C_{12})_2$Im][$FeCl_3Br$] were grown by allowing the compound to melt during the day and recrystallize overnight. Crystal selection was executed in the morning while the temperature was lower than 25 °C. It was observed that the focused light from the microscope accelerated the melting of the material. To combat this issue, two crystallization dishes were utilized in a "matryoshka doll" fashion. The inner dish held the microscope slide with the compound while the outer dish held ice to maintain cool temperatures. Melting was not observed using this method. A suitable crystal was found and immediately mounted on the goniometer head below a nitrogen cold stream at –183 °C. We attempted to

obtain crystals of the other materials with suitable melting points, $[(C_2)_2Im][FeCl_3Br]$, $[(C_{12})_2Im][FeCl_3Br]$, $[C_2C_1Im][FeCl_3Br]$, and $[C_{12}C_1Im][FeCl_3Br]$ using appropriate refrigerators or freezers, but were unsuccessful at this time.

The structure is found in the monoclinic setting with space group $P2_1/c$, Z = 4. The asymmetric unit is composed of the salt, $[(C_{12})_2Im][FeCl_3Br]$, illustrated in Figure 9. The cation is fully ordered. The anion shows disorder between the Br and Cl sites. Full refinement details are provided in the CIF (Supporting Information). The structure shows channels of $[FeCl_3Br]^-$ anions between sheets of $[(C_{12})_2Im]^+$ as shown in Figures 10 and 11. These channels are similar to those seen with other tetrahaloferrate(III) structures. We attempted to produce a different polymorph of $[(DD)_2Im][FeCl_3Br]$ by growing crystals in a refrigerator (4 °C), under the 1.5 T field of an $Nd_2Fe_{14}B$ magnet, and within the aligned field of two 1.5 T $Nd_2Fe_{14}B$ magnets. Much to our chagrin, the crystals obtained from these methods were the same form as the room temperature structure. Interestingly, the crystals obtained under magnetic influence were considerably better in quality. It is also noteworthy that the structure is devoid of solvent and water.

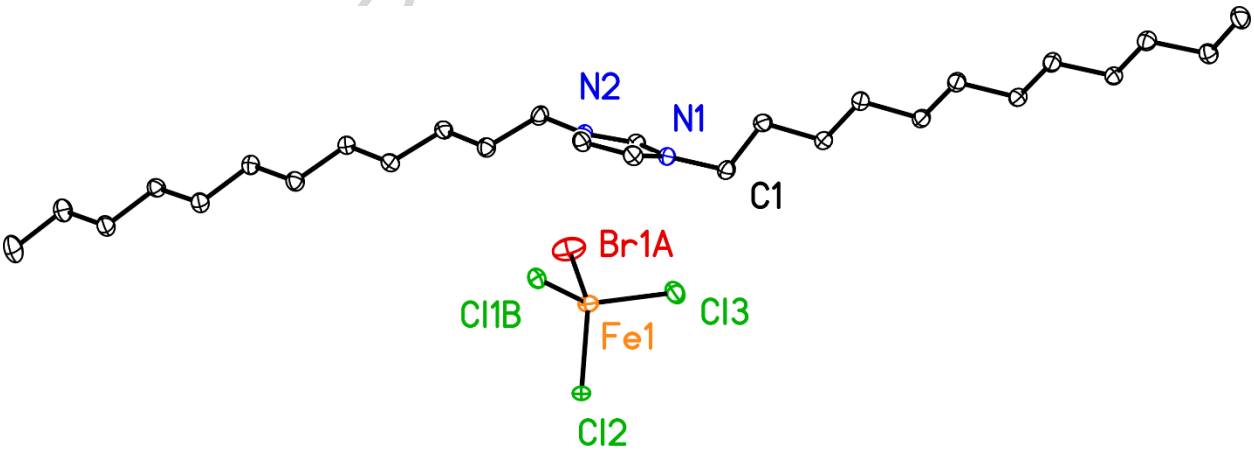

Figure 9. The asymmetric unit of $[(C_{12})_2Im][FeCl_3Br]$ drawn with 50% thermal contours. Hydrogen atoms and minor sites for Br and Cl are omitted for clarity. The color scheme is as follows: red =

bromine, green = chlorine, orange = iron, blue = nitrogen, black = carbon. Hydrogen atoms are omitted for clarity.

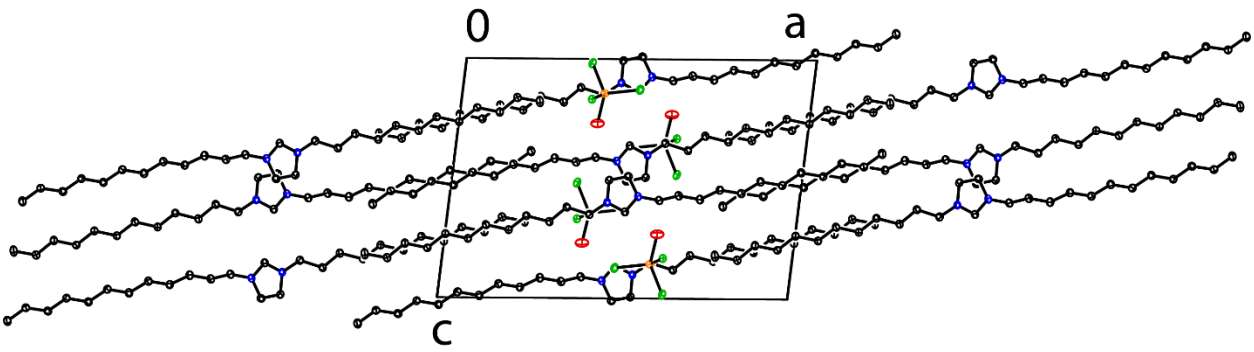

Figure 10. The packing diagram for the crystal structure $[(C_{12})_2Im][FeCl_3Br]$ looking down the crystallographic *b* axis. The color scheme is as follows: red = bromine, green = chlorine, orange = iron, blue = nitrogen, black = carbon. Hydrogen atoms are omitted for clarity.

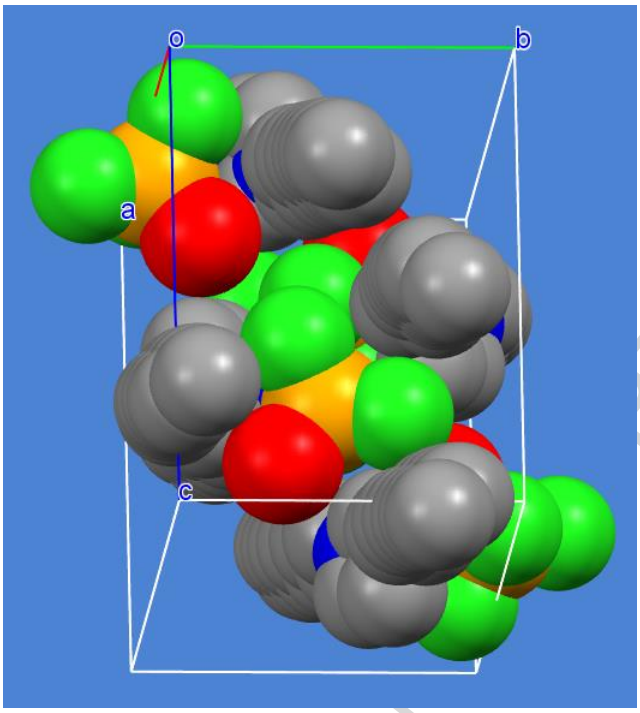

Figure 11. Space-filling model for $[(C_{12})_2Im][FeCl_3Br]$. The color scheme is as follows: red = bromine, green = chlorine, orange = iron, blue = nitrogen, grey = carbon. Hydrogen atoms are omitted for clarity.

Reaction Thermodynamic Calculations

Theoretical calculations of the gas phase enthalpies and free energies of reaction were performed for the PIL synthesis reactions:

$$[(C_n)_2Im][Br] + FeCl_3 \bullet 6H_2O \rightarrow [(C_n)_2Im][FeCl_3Br] + 6H_2O \quad \text{(Eq. 3)}$$

and:

$$[C_nC_1\ Im][Br] + FeCl_3 \bullet 6H_2O \rightarrow [C_nC_1Im][FeCl_3Br] + 6H_2O \quad \text{(Eq. 4)}$$

with the results summarized in Table 3. All of the computed reaction enthalpies (free energies) are endothermic (exergonic) and, with the exception of symmetric n-butyl $[(C_4)_2Im]^+$, are largely independent of alkyl chain length. The release of six product water molecules from the starting

$FeCl_3$•$6H_2O$ complex provides an increase in entropy, consistent with the predicted exergonicity of these reactions. The predicted endothermicity and exergonicity is qualitatively consistent with the corresponding experimental synthesis, for which the reactions proceed spontaneously but absorb heat.

Table 3. M06/aPCseg-2//M06/PCseg-2 gas-phase enthalpies and free energies of reactions shown in Equations 3 and 4 in kJ mol^{-1}.

[C_nC_1Im][$FeCl_3Br$]; *n*	ΔH_{rxn}^{298}	ΔG_{rxn}^{298}
2	79.3	-106.0
4	71.5	-111.5
6	68.9	-104.0
8	71.3	-112.4
10	71.3	-109.9
12	71.3	-110.7
[$(C_n)_2$Im][$FeCl_3Br$]; *n*		
2	58.7	-100.9
4	92.6	-96.6
6	67.0	-116.7
8	67.3	-116.3
10	52.1	-117.9
12	68.2	-122.1

CONCLUSION

Two series of alkyl-substituted imidazolium-based paramagnetic room temperature ionic liquids show promise as candidates for new types of paramagnetic ionic liquid applications that require short-term thermal stability above 300 °C in air while retaining low viscosity and surface tension characteristics. Contrary to expectations, both series show comparable melting points, with both

symmetrically and asymmetrically substituted compounds exhibiting melting points at a or below room temperature. Analysis of the X-ray crystal structure of one of these compounds indicates that disruption of crystalline order by bulky $[FeCl_3Br]^-$ anions may contribute to the observed low melting points. The ability to retain room temperature ionic liquid characteristics with both asymmetric and symmetric substitution patterns substantially increases the range of physical properties available by providing for a greater range of linear alkyl content. The greater linear alkyl content only modestly impacts the thermochemical stability of these compounds, with 5% weight loss temperatures in air becoming relatively independent of alkyl chain length and exceeding 320 °C for the longest chain lengths studied. In addition, surface energy is significantly reduced as alkyl chain length is increased. Density functional theory predictions of the reaction enthalpies and free energies for the formation of the PILs show these reactions to be entropically-driven and surprisingly independent of alkyl chain length. In combination with magnetic properties that were confirmed to be typical for imidazolium-based paramagnetic ionic liquids, these compounds afford performance with the potential to enable new applications in demanding thermal environments.

EXPERIMENTAL

General Considerations.

All solvents and reagents were obtained commercially and used as received with the exception of tetrahydrofuran (THF), diethyl ether, and toluene which were dried, deoxygenated, and stored on a solvent purification system similar to that described by Pangborn and Grubbs.[39] NMR solvents were dried and stored using appropriate molecular sieves. All reactions were performed

under an atmosphere of dry nitrogen, unless otherwise specified. After preparation, NaIm, $[(C_n)_2Im]Br$, $[C_nC_1Im]Br$, $[(C_n)_2Im][FeCl_3Br]$, and $[C_nC_1Im][FeCl_3Br]$ compounds were stored in a desiccator under a blanket of nitrogen. In addition, NaIm was stored in an amber bottle. Elemental analysis was conducted by Atlantic Microlab, Inc.

Spectroscopic Measurements.

^1H and ^{13}C NMR data were collected on a Bruker Avance III HD 400 MHz spectrometer using either $CDCl_3$ or DMSO-d_6 as solvent. Chemical shifts were referenced with respect to solvent. The intermediate $[(C_n)_2Im]Br$ and $[C_nC_1Im]Br$ compounds agree with literature NMR values. IR data were collected on a Nicolet iS50 FTIR spectrometer equipped with an ATR accessory. Spectra are shown in Supporting Information. UV-vis-NIR absorption data were recorded on a Shimadzu UV-3101PC spectrophotometer from 190-1100 nm. The expected signals at 534, 619, and 688 nm for the $[FeCl_3Br]^-$ anion were observed for all corresponding compounds.[26]

High-resolution Mass Spectrometry (HRMS).

HRMS was performed using ESI-Q-TOF-MS. Data were acquired using a Waters Synapt High Definition Mass Spectrometer equipped with a non-ESI source in positive and negative modes employing acetonitrile or methanol as solvent. MS conditions are as follows: capillary voltage (3.0 kV), sample cone voltage (33.0 V), extraction cone voltage (4.0 V), flow rate (1.000 nL/min), acquisition range (m/z 100-700), source temperature (80 °C).

Physical and Thermal Properties Measurements.

DSC data were recorded on a TA Instruments Q200 differential scanning calorimeter using a heat/cool/heat cycle with temperature limits of –85 and 175 °C, a heating rate of 10 °C/min, and a cooling rate of 5 °C/min. TGA data were recorded in air on a TA Instruments Q5000 from 40 to 600 °C with a heating rate of 5 °C/min. Additional TGA experiments using a heating rate of 10 °C/min are located in Supporting Information. Melting points were determined via DSC and verified via visual melting point determination when possible. Density was measured on a Rudolph Research Analytical DDM 2911 density meter at 25 °C. Kinematic viscosity was measured using a SCHOTT CT-52 capillary viscometer at 25 °C. Surface tension was measured using acquisition of a silhouette of the axisymmetric pendant fluid droplet.[34-35] Iterative fitting of the Young–Laplace equation was used to balance the gravitational deformation of the drop with the restorative interfacial tension. A Future Digital Scientific Corporation, Optical Contact Angle System (OCA-20) was used to capture silhouette images of the ionic liquid pendant drops in air, within a temperature-controlled chamber at 25 °C. Three separate images of each IL were analyzed using the open source software package Open Drop v1.1.

Single-Crystal X-ray Diffraction Experiment.

Crystals of $[(C_{12})_2Im][FeCl_3Br]$ were prepared and selected as outlined above (Results and Discussion). A brown plate was immediately mounted in the 90 K cold stream provided by a Cryo Industries low-temperature apparatus on the goniometer head of a Bruker ApexII CCD instrument employing Cu K_α (λ = 1.54056 Å) radiation. Data were reduced using Bruker SAINT, and a multi-scan absorption correction was applied using SADABS.[40] Structure solution and

refinement were executed on SHELXT-2015 and SHELXL-2017, respectively.[41-42] Crystallographic data are reported in the Supporting Information. Refinement details are provided in the CIF.

Computational Methods.

Density functional theory (DFT) methods were utilized to compute the gas phase enthalpies and free energies of the reactions of the imidazolium bromide ion pairs, $[(C_n)_2Im]Br$ and $[C_nC_1Im]Br$, with $FeCl_3•6H_2O$ to produce $[(C_n)_2Im][FeCl_3Br]$ and $[C_nC_1 Im][FeCl_3Br]$ plus $6H_2O$ molecules. The Lebedev quadrature scheme with 250 radial and 1454 angular grid points was used for DFT numerical integration. The structures of all reactants and products were fully optimized and confirmed as local minima via diagonalization of the mass-weighted matrix of energy second derivatives with respect to nuclear displacements; i.e., the hessian matrix. Harmonic vibrational frequencies were scaled by 0.983[43-44] in obtaining zero point vibrational energy corrections. The M06[43-44] meta-generalized gradient approximation (meta-GGA) functional was used in combination with the segmented polarization consistent basis set (PCseg-2).[45] Relative energies were refined via single point energy calculations using the augmented extension of the PCseg-2 basis set, denoted as M06/aPCseg-2//M06/PCseg-2. Spin unrestricted methods were used in computing the sextet electronic spin states of iron-containing species $FeCl_3•6H_2O$ and $[(C_n)_2Im][FeCl_3Br]$. All computations were performed using the GAMESS[46-47] quantum chemistry code.

Synthesis.

The [$(C_n)_2$Im]Br compounds can prepared according to literature methods.[22] However, we utilized an alternative synthesis path using NaIm as shown in Scheme 1. NaIm was prepared using imidazole and sodium hydroxide according to a literature procedure that was not modified.[25] The reaction of NaIm with two equivalents of alkyl bromide took place in THF under an atmosphere of nitrogen, outlined in detail below, using a modified work-up procedure to what was previously published. The [C_nC_1Im]Br compounds were prepared according to literature methods. NMR data for the [$(C_n)_2$Im]Br and [C_nC_1Im]Br series agree with the literature.[22] The [$(C_n)_2$Im][$FeCl_3Br$] series were prepared neat for C_n = 2, 4, 6, 8, 10 according to literature methods.[19, 31] For [$(C_{12})_2$Im][$FeCl_3Br$] methanol was used as a solvent since the product is a solid.[26] The entire [C_nC_1Im][$FeCl_3Br$] series was prepared neat. The characteristic visible spectroscopy bands at 534, 619, and 688 nm were observed for $[FeCl_3Br]^-$.[26] In addition, samples were submitted for EA and/or HRMS as required.

[$(C_2)_2$Im]Br. To a round-bottom flask equipped with a reflux condenser and magnetic stir bar, NaIm (5.032 g, 55.87 mmol) was suspended in 100 mL THF. 1-Bromoethane (5.5 eq., 32.967 g, 302.56 mmol) was added to this stirred, yellow suspension. This mixture was refluxed for 24 hours and then allowed to cool to room temperature. The reaction mixture, containing a light yellow liquor with off-white solids (NaBr), was filtered and washed with ca. 150 mL THF. Solvent was removed via rotary evaporation and the resulting yellow oil was dissolved in dichloromethane. This solution was filtered, solvent removed via rotary evaporation, and then stirred vigorously with ca. 150 mL diethyl ether. The diethyl ether was removed via cannulation because the low viscosity of the product did not allow for decantation. The washing step with

diethyl ether was repeated twice, and solvent was removed from the final yellow oil by rotary evaporation followed by vacuum line (10^{-2} torr). Yield: yellow oil, 5.327 g, 46.5 %.

[$(C_4)_2$Im]Br. This was prepared similarly to [$(C_2)_2$Im]Br using NaIm (4.018 g, 44.62 mmol) and 1-bromobutane (14.021 g, 102.3 mmol). Yield: yellow oil, 9.250 g, 79.4%.

[$(C_6)_2$Im]Br. This was prepared similarly to [$(C_2)_2$Im]Br using NaIm (4.004 g, 44.47 mmol) and 1-bromohexane (15.441 g, 93.53 mmol). Yield: yellow oil, 12.241 g, 86.74%.

[$(C_8)_2$Im]Br. This was prepared similarly to [$(C_2)_2$Im]Br using NaIm (4.660 g, 51.74 mmol) and 1-bromooctane (20.105 g, 104.11 mmol). Yield: yellow oil, 10.637 g, 55.1%.

[$(C_{10})_2$Im]Br. This was prepared similarly to [$(C_2)_2$Im]Br using NaIm (4.050 g, 44.97 mmol) and 1-bromodecane (20.020 g, 90.51 mmol). Yield: white foam-like solid, 11.170 g, 57.80%.

[$(C_{12})_2$Im]Br. This was prepared similarly to [$(C_2)_2$Im]Br using NaIm (3.522 g, 39.11 mmol) and 1-bromododecane (19.277 g, 77.35 mmol). Yield: white solid, 10.817 g, 57.6%.

[$(C_2)_2$Im][$FeCl_3Br$]. A 100 mL round-bottom flask with a magnetic stir bar was charged with [$(C_2)_2$Im]Br (5.327 g, 25.97 mmol) and $FeCl_3 \bullet 6H_2O$ (7.021 g, 25.97 mmol). The mixture immediately turned into a viscous red-brown liquid and was flushed with nitrogen for five minutes. The reaction was stirred overnight. Water was removed *in vacuo*, forming the product

in near-quantitative yield. After back-filling with nitrogen, the product was stored in a desiccator. Mp: –0.1 °C. HRMS (ESI/Q-TOF) *m*/*z*: [M^+] Calcd for $C_7H_{13}N_2$ 125.1079; Found: 125.1072. [M^-] Calc. for $FeCl_3Br$ 239.7598; Found: 239.7681. EA Calcd (%) for $C_7H_{13}N_2FeCl_3Br$: C, 22.89; H, 3.57; N, 7.63. Found: C, 22.60; H, 3.48; N, 7.41.

[$(C_4)_2$Im][$FeCl_3Br$]. This was prepared similarly to [$(C_2)_2$Im][$FeCl_3Br$] using [$(C_4)_2$Im]Br (4.831 g, 18.50 mmol) and $FeCl_3$•$6H_2O$ (5.026 g, 18.59 mmol). Near-quantitative yield, red-brown viscous liquid. HRMS (ESI/Q-TOF) *m*/*z*: [M^+] Calcd for $C_{11}H_{21}N_2$ 181.1705; Found: 181.1703. EA Calcd (%) for $C_{11}H_{21}N_2FeCl_3Br$: C, 31.20; H, 5.00; N, 6.62. Found: C, 31.28; H, 5.12; N, 6.87.

[$(C_6)_2$Im][$FeCl_3Br$]. This was prepared similarly to [$(C_2)_2$Im][$FeCl_3Br$] using [$(C_6)_2$Im]Br (3.301 g, 10.40 mmol) and $FeCl_3$•$6H_2O$ (2.857 g, 10.57 mmol). Near-quantitative yield, red-brown viscous liquid. HRMS (ESI/Q-TOF) *m*/*z*: [M^+] Calcd for $C_{15}H_{29}N_2$ 237.2331; Found: 237.2332. EA Calcd (%) for $C_{15}H_{29}N_2FeCl_3Br$: C, 37.57; H, 6.10; N, 5.84. Found: C, 38.17; H, 6.37; N, 5.16.

[$(C_8)_2$Im][$FeCl_3Br$]. This was prepared similarly to [$(C_2)_2$Im][$FeCl_3Br$] using [$(C_8)_2$Im]Br (10.637 g, 28.47 mmol) and $FeCl_3$•$6H_2O$ (7.986 g, 29.54 mmol). Near-quantitative yield, red-brown viscous liquid. HRMS (ESI/Q-TOF) *m*/*z*: [M^+] Calcd for $C_{19}H_{37}N_2$ 293.2957; Found: 293.2959. EA Calcd (%) for $C_{19}H_{37}N_2FeCl_3Br$: C, 42.61; H, 6.96; N, 5.23. Found: C, 42.35; H, 7.15; N, 5.16.

[$(C_{10})_2$Im][$FeCl_3Br$]. This was prepared similarly to [$(C_2)_2$Im][$FeCl_3Br$] using [$(C_{10})_2$Im]Br (11.170 g, 26.01 mmol) and $FeCl_3$•$6H_2O$ (7.023 g, 26.01 mmol). Near-quantitative yield, red-brown viscous

liquid. Mp: 4.6 °C. HRMS (ESI/Q-TOF) *m*/*z*: [M^+] Calcd for $C_{23}H_{45}N_2$ 349.3583; Found: 349.3596. EA Calcd (%) for $C_{23}H_{45}N_2FeCl_3Br$: C, 46.69; H, 7.67; N, 4.73. Found: C, 46.62; H, 7.67; N, 4.76.

[$(C_{12})_2$Im][$FeCl_3$Br]. A flask was charged with [$(C_{12})_2$Im]Br (10.134 g, 20.87 mmol) and $FeCl_3$•$6H_2O$ (5.574 g, 20.62 mmol). The mixture immediately turned into a red-brown liquid. Methanol (25 mL) was added and the reaction was stirred while flushing with nitrogen for five minutes. The mixture was stirred for an additional 8 hours. Solvent and water were then removed *in vacuo*. Quantitative yield, red-brown viscous liquid. *Note*: Depending on laboratory temperature, the product can solidify. Mp: 25.1 °C. HRMS (ESI/Q-TOF) *m*/*z*: [M^+] Calc. for $C_{27}H_{53}N_2$ 405.4209; Found: 405.4210. EA Calcd (%) for $C_{27}H_{53}N_2FeCl_3Br$: C, 50.06; H, 8.25; N, 4.32. Found: C, 50.16; H, 8.61; N, 4.65.

[C_2C_1Im][$FeCl_3$Br]. This was prepared similarly to [$(C_2)_2$Im][$FeCl_3$Br] using [C_2C_1Im]Br (11.233 g, 58.79 mmol) and $FeCl_3$•$6H_2O$ (15.851 g, 58.64 mmol). Near-quantitative yield, red-brown viscous liquid. Mp: 19.4 °C. HRMS (ESI/Q-TOF) *m*/*z*: [M^+] Calcd for $C_6H_{11}N_2$ 111.0922; Found: 111.0926. EA Calcd (%) for $C_6H_{11}N_2FeCl_3Br$: C, 20.40; H, 3.14; N, 7.93. Found: C, 20.48; H, 3.18; N, 7.69.

[C_4C_1Im][$FeCl_3$Br]. This was prepared similarly to [$(C_2)_2$Im][$FeCl_3$Br] using [C_4C_1Im]Br (3.473 g, 15.85 mmol) and $FeCl_3$•$6H_2O$ (4.285 g, 15.85 mmol). Near-quantitative yield, red-brown viscous liquid. HRMS (ESI/Q-TOF) *m*/*z*: [M^+] Calcd for $C_8H_{15}N_2$ 139.1235; Found: 139.1229. EA Calcd (%) for $C_8H_{15}N_2FeCl_3Br$: C, 25.20; H, 3.96; N, 7.35. Found: C, 24.73; H, 3.85; N, 7.10.

[C_6C_1Im][$FeCl_3$Br]. This was prepared similarly to [$(C_2)_2$Im][$FeCl_3$Br] using [C_6C_1Im]Br (15.323 g, 61.99 mmol) and $FeCl_3$•$6H_2O$ (16.742 g, 61.94 mmol). Near-quantitative yield, red-brown viscous liquid. HRMS (ESI/Q-TOF) *m*/*z*: [M^+] Calcd for $C_{10}H_{19}N_2$ 167.1548; Found: 167.1540. EA Calcd (%) for $C_{10}H_{19}N_2FeCl_3Br$: C, 29.34; H, 4.68; N, 6.84. Found: C, 28.83; H 4.67; N, 6.63.

[C_8C_1Im][$FeCl_3$Br]. This was prepared similarly to [$(C_2)_2$Im][$FeCl_3$Br] using [C_8C_1Im]Br (17.836 g, 64.80 mmol) and $FeCl_3$•$6H_2O$ (17.503 g, 64.75 mmol). Near-quantitative yield, red-brown viscous liquid. HRMS (ESI/Q-TOF) *m*/*z*: [M^+] Calcd for $C_{12}H_{23}N_2$ 195.1861; Found: 195.1856. EA Calcd (%) for $C_{12}H_{23}N_2FeCl_3Br$: C, 32.95; H, 5.30; N, 6.40. Found: C, 32.35; H 5.37; N, 6.28.

[$C_{10}C_1$Im][$FeCl_3$Br]. This was prepared similarly to [$(C_2)_2$Im][$FeCl_3$Br] using [$C_{10}C_1$Im]Br (17.628 g, 58.12 mmol) and $FeCl_3$•$6H_2O$ (15.704 g, 58.10 mmol). Near-quantitative yield, red-brown viscous liquid. HRMS (ESI/Q-TOF) *m*/*z*: [M^+] Calcd for $C_{14}H_{27}N_2$ 223.2174; Found: 223.2165. EA Calcd (%) for $C_{14}H_{27}N_2FeCl_3Br$: C, 36.12; H, 5.85; N, 6.02. Found: C, 36.20; H 5.84; N, 6.07.

[$C_{12}C_1$Im][$FeCl_3$Br]. This was prepared similarly to [$(C_2)_2$Im][$FeCl_3$Br] using [$C_{12}C_1$Im]Br (18.709 g, 56.47 mmol) and $FeCl_3$•$6H_2O$ (15.220 g, 56.31 mmol). Near-quantitative yield, red-brown viscous liquid. Mp: 14.5 °C. HRMS (ESI/Q-TOF) *m*/*z*: [M^+] Calcd for $C_{16}H_{31}N_2$ 251.2487; Found: 251.2466. EA Calcd (%) for $C_{16}H_{31}N_2FeCl_3Br$: C, 38.94; H, 6.33; N, 5.78. Found: C, 39.14; H 6.33; N, 5.68.

ASSOCIATED CONTENT

Supporting Information. The Supporting Information is available free of charge online. Included are the FTIR spectra, DFT optimized structures as well as their Cartesian coordinates, crystallographic data table, TGA plots at 10 °C/min, water content for the $[(C_n)_2Im][FeCl_3Br]$ and $[C_nC_1Im][FeCl_3Br]$ compounds.

Accession Codes

CCDC 1825333 contains the supplementary crystallographic data for this paper. These data can be obtained free of charge via www.ccdc.cam.ac.uk/data_request/cif, or by emailing data_request@ccdc.cam.ac.uk, or by contacting The Cambridge Crystallographic Data Centre, 12 Union Road, Cambridge CB2 1EZ, UK; fax: +44 1223 336033.

AUTHOR INFORMATION

Corresponding Author.

*E-mail: kamran.ghiassi@us.af.mil

Notes.

The authors declare no competing financial interest.

ACKNOWLEDGMENTS

The support of the Air Force Office of Scientific Research and the Air Force Research Laboratory are gratefully acknowledged. The authors thank Mr. Brett Wight and Ms. Cassandra Alabada for verifying elemental analysis results and Dr. Yonis Ahmed for insightful discussion. A grant of

computer time from the Department of Defense High Performance Computing Modernization Program at the DoD Supercomputing Research Centers (DSRCs) located at the Army Research Laboratory, Navy, and Engineer Research and Development Center is gratefully acknowledged. Work at the Molecular Foundry was supported by the Office of Science, Office of Basic Energy Sciences, of the U.S. Department of Energy under Contract No. DE-AC02-05CH11231.

REFERENCES

1. Kuwabata, S.; Tsuda, T.; Torimoto, T., Room-Temperature Ionic Liquid. A New Medium for Material Production and Analyses under Vacuum Conditions. *The Journal of Physical Chemistry Letters* **2010,** *1* (21), 3177-3188.

2. Cao, Y.; Wu, J.; Zhang, J.; Li, H.; Zhang, Y.; He, J., Room temperature ionic liquids (RTILs): A new and versatile platform for cellulose processing and derivatization. *Chemical Engineering Journal* **2009,** *147* (1), 13-21.

3. Hallett, J. P.; Welton, T., Room-Temperature Ionic Liquids: Solvents for Synthesis and Catalysis. 2. *Chemical Reviews* **2011,** *111* (5), 3508-3576.

4. Martins, I. C. B.; Gomes, J. R. B.; Duarte, M. T.; Mafra, L., Understanding Polymorphic Control of Pharmaceuticals Using Imidazolium-Based Ionic Liquid Mixtures as Crystallization Directing Agents. *Cryst. Growth Des.* **2017**.

5. Vekariya, R. L., A review of ionic liquids: Applications towards catalytic organic transformations. *Journal of Molecular Liquids* **2017,** *227*, 44-60.

6. Martinez-Palou, R.; Luque, R., Applications of ionic liquids in the removal of contaminants from refinery feedstocks: an industrial perspective. *Energy & Environmental Science* **2014,** *7* (8), 2414-2447.

7. Likhanova, N. V.; Guzmán-Lucero, D.; Flores, E. A.; García, P.; Domínguez-Aguilar, M. A.; Palomeque, J.; Martínez-Palou, R., Ionic liquids screening for desulfurization of natural gasoline by liquid–liquid extraction. *Molecular Diversity* **2010,** *14* (4), 777-787.

8. Pereiro, A. B.; Araújo, J. M. M.; Martinho, S.; Alves, F.; Nunes, S.; Matias, A.; Duarte, C. M. M.; Rebelo, L. P. N.; Marrucho, I. M., Fluorinated Ionic Liquids: Properties and Applications. *ACS Sustainable Chemistry & Engineering* **2013,** *1* (4), 427-439.

9. Tian, T.; Hu, Q.; Wang, Y.; Gao, Y. a.; Yu, L., Effect of Imidazolium-Based Surface-Active Ionic Liquids on the Orientation of Liquid Crystals at Various Fluid/Liquid Crystal Interfaces. *Langmuir* **2016,** *32* (45), 11745-11753.

10. Joseph, A.; Żyła, G.; Thomas, V. I.; Nair, P. R.; Padmanabhan, A. S.; Mathew, S., Paramagnetic ionic liquids for advanced applications: A review. *Journal of Molecular Liquids* **2016,** *218*, 319-331.

11. De Vreese, P.; Brooks, N. R.; Van Hecke, K.; Van Meervelt, L.; Matthijs, E.; Binnemans, K.; Van Deun, R., Speciation of Copper(II) Complexes in an Ionic Liquid Based on Choline Chloride and in Choline Chloride/Water Mixtures. *Inorganic Chemistry* **2012,** *51* (9), 4972-4981.

12. Mallick, B.; Balke, B.; Felser, C.; Mudring, A.-V., Dysprosium Room-Temperature Ionic Liquids with Strong Luminescence and Response to Magnetic Fields. *Angewandte Chemie International Edition* **2008,** *47* (40), 7635-7638.

13. Mehdi, H.; Binnemans, K.; Van Hecke, K.; Van Meervelt, L.; Nockemann, P., Hydrophobic ionic liquids with strongly coordinating anions. *Chem. Commun.* **2010,** *46* (2), 234-236.

14. Nockemann, P.; Thijs, B.; Postelmans, N.; Van Hecke, K.; Van Meervelt, L.; Binnemans, K., Anionic Rare-Earth Thiocyanate Complexes as Building Blocks for Low-Melting Metal-Containing Ionic Liquids. *Journal of the American Chemical Society* **2006,** *128* (42), 13658-13659.

15. Del Sesto, R. E.; McCleskey, T. M.; Burrell, A. K.; Baker, G. A.; Thompson, J. D.; Scott, B. L.; Wilkes, J. S.; Williams, P., Structure and magnetic behavior of transition metal based ionic liquids. *Chem. Commun.* **2008,** (4), 447-449.

16. Taylor, A. W.; Licence, P., X-Ray Photoelectron Spectroscopy of Ferrocenyl- and Ferrocenium-Based Ionic Liquids. *ChemPhysChem* **2012,** *13* (7), 1917-1926.

17. Kogelnig, D.; Stojanovic, A.; v.d. Kammer, F.; Terzieff, P.; Galanski, M.; Jirsa, F.; Krachler, R.; Hofmann, T.; Keppler, B. K., Tetrachloroferrate containing ionic liquids: Magnetic- and aggregation behavior. *Inorganic Chemistry Communications* **2010,** *13* (12), 1485-1488.

18. Yoshida, Y.; Saito, G., Design of functional ionic liquids using magneto- and luminescent-active anions. *Physical Chemistry Chemical Physics* **2010,** *12* (8), 1675-1684.

19. Bwambok, D. K.; Thuo, M. M.; Atkinson, M. B. J.; Mirica, K. A.; Shapiro, N. D.; Whitesides, G. M., Paramagnetic Ionic Liquids for Measurements of Density Using Magnetic Levitation. *Analytical Chemistry* **2013,** *85* (17), 8442-8447.

20. Repper, S. E.; Haynes, A.; Ditzel, E. J.; Sunley, G. J., Infrared spectroscopic study of absorption and separation of CO using copper(i)-containing ionic liquids. *Dalton Transactions* **2017,** *46* (9), 2821-2828.

21. Sharma, R. K.; Chouryal, Y. N.; Chaudhari, S.; Saravanakumar, J.; Dey, S. R.; Ghosh, P., Adsorption-Driven Catalytic and Photocatalytic Activity of Phase Tuned In2S3 Nanocrystals Synthesized via Ionic Liquids. *ACS Appl. Mater. Interfaces* **2017,** *9* (13), 11651-11661.

22. Dzyuba, S. V.; Bartsch, R. A., New room-temperature ionic liquids with -symmetrical imidazolium cations. *Chem. Commun.* **2001,** (16), 1466-1467.

23. Liu, S.; Xu, T., Ionic Liquids Containing Block Copolymer Based Supramolecules. *Macromolecules* **2016,** *49* (16), 6075-6083.

24. Wang, W.-J.; Hu, M.-J.; Chang, C.-S.; Chuang, K.-S.; Chiu, H.-S.; Sheu, C.-F., Synthetic Conducting Materials. XIII. Charge Transfer Complexe of 1,3-di-hexadecanylimidazolium with TCNQ. *Synthetic Metals* **1999,** *102* (1–3), 1725-1726.

25. Bara, J. E., Versatile and Scalable Method for Producing N-Functionalized Imidazoles. *Industrial & Engineering Chemistry Research* **2011,** *50* (24), 13614-13619.

26. Nacham, O.; Clark, K. D.; Yu, H.; Anderson, J. L., Synthetic Strategies for Tailoring the Physicochemical and Magnetic Properties of Hydrophobic Magnetic Ionic Liquids. *Chemistry of Materials* **2015,** *27* (3), 923-931.

27. Satoshi, H.; Hiro-o, H., Discovery of a Magnetic Ionic Liquid [bmim]FeCl4. *Chemistry Letters* **2004,** *33* (12), 1590-1591.

28. Sitze, M. S.; Schreiter, E. R.; Patterson, E. V.; Freeman, R. G., Ionic Liquids Based on FeCl3 and FeCl2. Raman Scattering and ab Initio Calculations. *Inorganic Chemistry* **2001,** *40* (10), 2298-2304.

29. Zhou, C.; Yu, X.; Ma, H.; Huang, X.; Zhang, H.; Jin, J., Properties and catalytic activity of magnetic and acidic ionic liquids: Experimental and molecular simulation. *Carbohydrate Polymers* **2014,** *105*, 300-307.

30. Brown, P.; Bushmelev, A.; Butts, C. P.; Cheng, J.; Eastoe, J.; Grillo, I.; Heenan, R. K.; Schmidt, A. M., Magnetic Control over Liquid Surface Properties with Responsive Surfactants. *Angewandte Chemie International Edition* **2012,** *51* (10), 2414-2416.

31. Yoshida, Y.; Saito, G., Influence of structural variations in 1-alkyl-3-methylimidazolium cation and tetrahalogenoferrate(iii) anion on the physical properties of the paramagnetic ionic liquids. *Journal of Materials Chemistry* **2006,** *16* (13), 1254-1262.

32. Yoshida, Y.; Otsuka, A.; Saito, G.; Natsume, S.; Nishibori, E.; Takata, M.; Sakata, M.; Takahashi, M.; Yoko, T., Conducting and Magnetic Properties of 1-Ethyl-3-methylimidazolium (EMI) Salts Containing Paramagnetic Irons: Liquids $[EMI][M^{III}Cl_4]$ (M = Fe and $Fe_{0.5}Ga_{0.5}$) and Solid $[EMI]_2[Fe^{II}Cl_4]$. *Bulletin of the Chemical Society of Japan* **2005,** *78* (11), 1921-1928.

33. Gao, J.; Wang, J.-Q.; Song, Q.-W.; He, L.-N., Iron(iii)-based ionic liquid-catalyzed regioselective benzylation of arenes and heteroarenes. *Green Chemistry* **2011,** *13* (5), 1182-1186.

34. Berry, J. D.; Neeson, M. J.; Dagastine, R. R.; Chan, D. Y. C.; Tabor, R. F., Measurement of surface and interfacial tension using pendant drop tensiometry. *Journal of Colloid and Interface Science* **2015,** *454*, 226-237.

35. Di Nicola, G.; Pierantozzi, M., Surface tension of alcohols: A scaled equation and an artificial neural network. *Fluid Phase Equilibria* **2015,** *389*, 16-27.

36. Brown, P.; Bushmelev, A.; Butts, C. P.; Eloi, J.-C.; Grillo, I.; Baker, P. J.; Schmidt, A. M.; Eastoe, J., Properties of New Magnetic Surfactants. *Langmuir* **2013,** *29* (10), 3246-3251.

37. Zheng, W.; Mohammed, A.; Hines, L. G.; Xiao, D.; Martinez, O. J.; Bartsch, R. A.; Simon, S. L.; Russina, O.; Triolo, A.; Quitevis, E. L., Effect of Cation Symmetry on the Morphology and Physicochemical Properties of Imidazolium Ionic Liquids. *The Journal of Physical Chemistry B* **2011,** *115* (20), 6572-6584.

38. Nacham, O.; Clark, K. D.; Anderson, J. L., Synthesis and characterization of the physicochemical and magnetic properties for perfluoroalkyl ester and Fe(iii) carboxylate-based hydrophobic magnetic ionic liquids. *RSC Advances* **2016,** *6* (14), 11109-11117.

39. Pangborn, A. B.; Giardello, M. A.; Grubbs, R. H.; Rosen, R. K.; Timmers, F. J., Safe and Convenient Procedure for Solvent Purification. *Organometallics* **1996,** *15* (5), 1518-1520.

40. SAINT and SADABS, Bruker AXS, Inc.: Madison, WI, **2014**.

41. Sheldrick, G., SHELXT - Integrated space-group and crystal-structure determination. *Acta Crystallogr., Sect. A* **2015,** *71* (1), 3-8.

42. Sheldrick, G., Crystal structure refinement with SHELXL. *Acta Crystallogr., Sect. C* **2015,** *71* (1), 3-8.

43. Zhao, Y.; Truhlar, D. G., Density Functionals with Broad Applicability in Chemistry. *Acc. Chem. Res.* **2008,** *41* (2), 157-167.

44. Zhao, Y.; Truhlar, D. G., The M06 suite of density functionals for main group thermochemistry, thermochemical kinetics, noncovalent interactions, excited states, and transition elements: two new functionals and systematic testing of four M06-class functionals and 12 other functionals. *Theor. Chem. Acc.* **2008,** *120* (1), 215-241.

45. Jensen, F., Unifying General and Segmented Contracted Basis Sets. Segmented Polarization Consistent Basis Sets. *Journal of Chemical Theory and Computation* **2014,** *10* (3), 1074-1085.

46. Gordon, M. S.; Schmidt, M. W., Chapter 41 - Advances in electronic structure theory: GAMESS a decade later A2 - Dykstra, Clifford E. In *Theory and Applications of Computational Chemistry*, Frenking, G.; Kim, K. S.; Scuseria, G. E., Eds. Elsevier: Amsterdam, 2005; pp 1167-1189.

47. Schmidt, M. W.; Baldridge, K. K.; Boatz, J. A.; Elbert, S. T.; Gordon, M. S.; Jensen, J. H.; Koseki, S.; Matsunaga, N.; Nguyen, K. A.; Su, S.; Windus, T. L.; Dupuis, M.; Montgomery, J. A., General atomic and molecular electronic structure system. *J. Comput. Chem.* **1993,** *14* (11), 1347-1363.

48. Maton, C.; De Vos, N.; Stevens, C. V. Ionic liquid thermal stabilities: decomposition mechanisms and analysis tools. *Chem. Soc. Rev.* **2013**, *42*, 5963-5977.

TOC Graphic

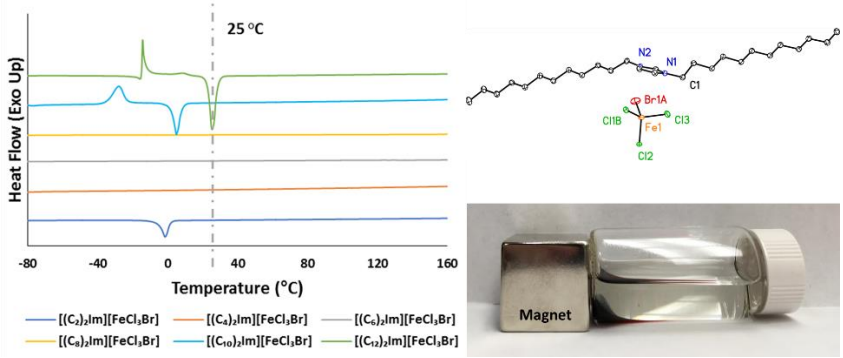

Graphical abstract

Highlights

- Synthesis of new paramagnetic, room temperature ionic liquids with high short-term thermal stability
- Symmetrically-alkylated imidazolium cations paired with bromotrichloroferrate(III) anions
- All compounds in this study have high thermal stabilities greater than or equal to 300 °C in air
- All compounds in this study have melting points less than or equal to room temperature (25 °C)
- Paramagnetic ionic liquids in this study can be manipulated by external magnetic field